Low Temperature Physics/Fizika Nizkikh Temperatur, 2013, v. 39, No. 5, pp. 574–579

Anomalous low-temperature “post-desorption” from solid nitrogen

E.V. Savchenko[1], I.V. Khyzhniy[1], S.A. Uyutnov[1], A.N. Ponomaryov[3], G.B. Gumenchuk[2], and V.E. Bondybey[2]

[1]*B. Verkin Institute for Low Temperature Physics and Engineering of the National Academy of Sciences of Ukraine*
47 Lenin Ave., Kharkov 61103, Ukraine
E-mail: elena.savchenko@gmail.com

[2]*Lehrstuhl für Physikalische Chemie II TUM, Garching b. München 85747, Germany*

[3]*Helmholtz Zentrum Dresden-Rossendorf, Dresden 01328, Germany*

Received February 1, 2013

Anomalous low-temperature post-desorption (ALTpD) from the surface of nominally pure solid nitrogen preliminary irradiated by an electron beam was detected for the first time. The study was performed using a combination of activation spectroscopy methods — thermally stimulated exoelectron emission (TSEE) and spectrally resolved thermally stimulated luminescence (TSL) — with detection of the ALTpD yield. Charge recombination reactions are considered to be the stimulating factor for the desorption from pre-irradiated α-phase solid nitrogen.

PACS: *66.30.hp* Molecular crystals;
79.20.La Photon- and electron-stimulated desorption.

Keywords: solid nitrogen, exoelectron emission, thermoluminescence, desorption.

1. Introduction

Thermal desorption of atomic and molecular species from different substrates and solidified gas layers has attracted much attention ([1–12] and references therein) for its intrinsic scientific merits and numerous technological applications (surface modification, nanochemistry, storage of gases in nanostructured materials, vacuum technique, etc.). Molecules or atoms adsorbed on a surface have different binding energies which vary with sites at the surface. When the surface is heated the energy transferred to the adsorbed species at some temperature appears large enough to break the bond and cause the adsorbate desorption. Temperature-programmed desorption (TPD) technique is in most common use to study the binding energies, kinetic and thermodynamic parameters of desorption. The partial pressures of atoms or molecules desorbing from the sample upon heating by a certain program are measured, e.g., by mass spectrometry, yielding fluxes of species as a function of temperature. The temperature at which desorption takes place is characteristic of adsorbate and the position of its adsorption. Because of this TPD technique is often called thermal desorption spectroscopy (TDS). The intensity of TDS peaks provides information on the amounts of species adsorbed at different sites of the surface. So, studying the low-temperature desorption of nitrogen from the N_2-saturated powder of bundles of single-walled carbon nanotubes (SWCNTs) with open and closed ends [1] it was shown that high concentration of N_2 can be sorbed especially by tubes with open ends (up to 46.4 mol/mol%) and the sites of possible sorption of N_2 molecules were found. It was suggested that N_2 molecules can occupy the grooves at the surface of SWNT bundles and form two or three layers at the bundle surface. They can also penetrate through inevitable surface defects inside the nanotubes that form the outer surface of the bundle.

Special attention is paid to thermal desorption in studies of interstellar ice analogues [2,6,11,12]. Survey of laboratory study of the thermal desorption of astrophysically relevant molecules is presented in [11]. The desorption behavior of monolayers and multilayers of N_2, O_2, CO, CH_4 and other molecules during thermal processing was investigated with TPD/TDS technique. Desorption peak of nitrogen deposited on to a gold substrate was observed near 20 K. Note that TPD trace of nitrogen deposited on to a pre-adsorbed films of solid H_2O differs greatly in shape.

Several peaks were observed near 25, 45, 140 and 160 K. Desorption of nitrogen from SWCNTs [1] showed two wide peaks about 50 and 75 K.

Another type of desorption or sputtering is observed under excitation with high-energy photons, electrons and ions. In this case the physical processes caused the sputtering of mono- and multilayers are, so-called, knock-on collisions and electronic excitations. If an energetic incident particle strikes the surface a target particle may gain sufficient momentum to overcome the binding forces and escape directly or after a cascade of collisions. At relatively high beam fluxes the surface temperature increases and thermal desorption may also contribute to the sputtering yield. Electronic desorption or desorption induced by electronic transitions (DIET) is a more complex process involving relaxation of electronic excitations and conversion of electronic energy into atomic motions [13,14].

Electronic desorption of solid nitrogen was studied under excitation with electrons [15–20], ions [20–26] and photons [27,28]. Mass spectrometry analysis [16] of species desorbing under bombardment by 0.5 keV electrons revealed atoms, molecules and clusters ejected into vacuum: N, N_2, N_3, and N_4. The dominant component appeared to be N_2 molecules. Kinetic energy distribution of N and N_2 shows only one peak [16,17] with maximum near (29±4) meV for N_2 and (85±15) meV for N species [17]. As to mechanisms of electronically induced desorption from solid nitrogen they are still not well understood. Several mechanisms of DIET were considered. Based on kinetic energy distribution of particles desorbed from solid nitrogen it was suggested [16] that the relaxation energy is released in steps. An existence of two different parts, the high-energy tail from 1 to 3 eV and low-energy part below 1 eV, suggests at least two different nonradiative processes that cause DIET of solid nitrogen irradiated by an electron beam. As it was found in the experiments on determination of the threshold energy E_{thr} for electron stimulated desorption, E_{thr} of neutral molecules N_2 with respect to the conduction band is 6.8 eV [17]. Authors associate this threshold with low-laying triplet excitations $A^3\Sigma_u^+$. According their data the DIET cross-section is roughly proportional to that of the net electronic excitation. However no selective enhancement was found only some blurred step near 15 eV. DIET excited via negative ion resonances below the triplet threshold was registered with the extremely low yield (lower by a factor of 20 than that for DIET near the triplet threshold). Discussing different possible routs of excited state coupling to nuclear motion authors came to conclusion that coupling of electronic to translational energy through radiationless decay could be an important channel for DIET from molecular solids.

The primary excitations appearing under irradiation relax by different paths producing a number of secondary excitations and involve such processes as emission of electrons and photons, charge and energy transport, electron–hole recombination, creation of neutral and charged defect centers, mass diffusion, electronic desorption, radiation-induced reactions, etc. Some of secondary excitations are stabilized in the solid storing part of energy absorbed during irradiation. During the controlled warm-up this energy can be released as photons, electrons and spent partially for desorption. Recently [29–32] we found anomalous low-temperature post-desorption (ALTpD) of own atoms from the surfaces of pre-irradiated atomic cryocrystals. Strong peaks of atom ejection were observed at temperatures much lower than the characteristic sublimation temperature. Here we report first results of experiments on post-desorption of nitrogen from the surface of nominally pure solid nitrogen preliminary irradiated by an electron beam. Relaxation processes were monitored using a combination of three activation spectroscopy methods — thermally stimulated luminescence (TSL) and thermally stimulated exoelectron emission (TSEE) — with measurements of the desorption yield via pressure detection.

2. Experimental section

The experiments presented here were performed using facilities at TUM and ILT. The experimental techniques developed have been described in more detail in [30,33], and are therefore only briefly discussed here. Using the TSEE method in a desorption study is obviously preferable in comparison with other current activation spectroscopy methods because TSEE yield provides information on electron traps essentially on the surface and in the subsurface layers. TSL yield contains contributions from the relaxation processes both occurring in the sample bulk and in the subsurface layers. The developed approach enables us to measure simultaneously the TSEE yield, the total and partial yields of the TSL in the visible, near infrared, near UV and VUV ranges as well as to monitor and record the pressure above the sample, in a real time correlated fashion.

The samples were grown from the gas phase by deposition on a metal substrate coated by a thin layer of MgF_2, which was cooled to about 7 K by a two stage, closed-cycle Leybold RGD 580 refrigerator or a liquid helium cryostat. High-purity (99.999%) N_2 gas was used. The base pressure in the vacuum chamber was about 10^{-8} mbar. The deposition rate and the sample thickness were determined by observing the pressure decrease in a known volume of the gas-handling system. The typical deposition rate was about 10^{-1} μm/s, and samples of thickness 100 μm were grown.

In order to ionize the samples and produce charge centers we used slow electrons of 500 eV energy. The deposition was performed with a concurrent irradiation by electrons to generate charge centers throughout the sample or alternatively the sample was irradiated after deposition. The current density was kept at 30 μA/cm^2. An electrostatic lens was used to focus the electrons. The radiation dose

was varied by an exposure time. In the experiments presented we measured yields of TSEE from the samples, TSL in VUV range and pressure above the sample during sample heating. The exoelectron yield was measured with an electrode kept at a small positive potential +9 V and connected to the current amplifier FEMTO DLPCA 200. The VUV cathodoluminescence spectra in the range 50–300 nm were recorded with a modified VMR-2 monochromator. The pressure changes in the sample chamber during the experiment were monitored using a Compact BA Pressure Gauge PBR 260. For calibration we used a flow rate controller.

The temperature was measured by a calibrated silicon diode sensor mounted directly on the substrate, with the programmable temperature controller LTC 60 allowing us not only to measure and maintain any desired temperature during sample deposition, annealing and irradiation, but also to control the heating regime flexibly. The relaxation processes in N_2 samples were studied in the temperature range from 7 to 45 K. The entire control of the experiment and the simultaneous acquisition of the TSL and TSEE yields, as well as measurement and recording of the sample temperature and of the vacuum sample chamber pressure were accomplished using a computer program developed specifically for these studies.

3. Results and discussion

In contrast to the relaxation scenario under excitation the "post-irradiation" relaxation is triggered by controlled heating of the preliminary irradiated sample. Primary electronic states in this case are determined by stable centers survived in the solid on completing irradiation. Recent experiments [34] revealed strong thermally stimulated exoelectron emission from pre-irradiated solid nitrogen layers, suggesting accumulation of negative charge in the solid. Note that in solid nitrogen there is no barrier for electrons to escape from the surface because of its negative electron affinity [35]. The experimental studies of the excess electron transport in solid nitrogen performed using a muon spin relaxation technique, which involves microscopic distances (10^{-6}–10^{-5} cm) and therefore practically free from the influence of crystal imperfection have demonstrated free-like transport of electrons in α phase of solid nitrogen [36]. The results of both studies [34,36] indicate trapping of electrons at crystal defects and suggest a prominent part played by radiation-induced charged species in the energy storage and relaxation processes.

We combined measurements of TSEE yield with pressure monitoring upon warm-up of the pre-irradiated nitrogen film. The corresponding curves are shown in Fig. 1. The TSEE curve exhibits two distinguishable features in low-temperature range peaked at 12 and 15 K and a shoulder near 20 K. Then TSEE current gradually decreases to 30 K. Wide multipeaked curve indicates that there is a near-

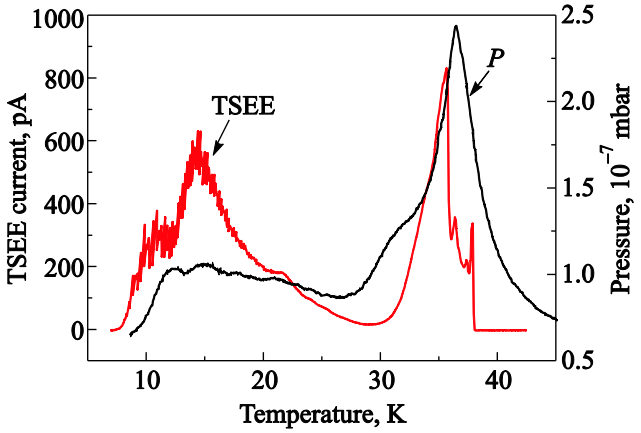

Fig. 1. Comparison of the electron emission yield with pressure behavior upon warm-up of the pre-irradiated with electrons film of solid nitrogen.

ly continuous distribution of trap energies. A shape of TSEE curve accounts for the structure of sample and depends on growth conditions. The most prominent peak is observed at 35 K. After 35.6 K where α–β phase transition occurs TSEE current falls off because of scattering of electrons on the rotational modes of N_2 in β phase. The pressure curve exhibits nonmonotonous behavior as illustrated in Fig. 1. Clear enhancement of the "post-desorption" was observed at low temperatures starting from 9 K with a wide peak near 15 K, that is much lower than the characteristic sublimation temperature of solid nitrogen T_{sb} = 37 K. Because of this feature this phenomenon will be called anomalous low-temperature post-desorption. The most striking feature of these curves is the correlation in pressure increase and yield of TSEE. Such a correlation points to connection of ALTpD with recombination of positively charged centers and electrons. Interesting that upon completing irradiation at low temperature some time was required to stabilize both pressure and current. Figure 2 illustrates a decrease of pressure and current (afteremission) after the electron beam was switched off. Again clear correlation of pressure behavior measured in the chamber and afteremission yield

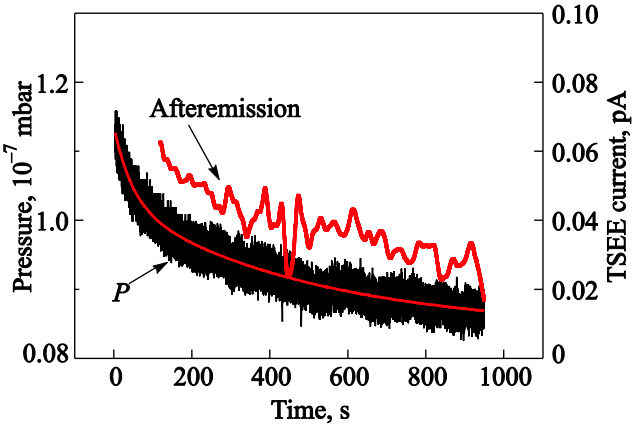

Fig. 2. Temporal behavior of pressure and afteremission of electrons from the pre-irradiated film of solid nitrogen.

was observed. Decay curve for pressure can be fitted by two exponentials with the characteristic times $\tau_1 = (30\pm5)$ s and $\tau_2 = (500\pm50)$ s.

It is well-known that solid nitrogen exhibits a long-lasting afterglow related to the forbidden atomic transition $^2D \rightarrow {}^4S$, so-called α group, with characteristic times 9–37 s which belong to different components of this group: $\tau = 9$ s (521 nm), $\tau = 25$ s (522 nm), $\tau = 37$ s (523 nm) [37]. In order to check the assumption that afteremission is stimulated by photons of α line we measured afterglow from pre-irradiated film of nitrogen on α line. The afterglow and its exponential fit are shown in Fig. 3. The characteristic times $\tau = (25\pm3)$ s appeared to be close to τ_1 extracted from the afteremission decay curve. Note that the spectral slit in this experiment was not narrow enough to resolve components of α group, so the magnitude obtained gives averaged τ. However the correlation of decay times for afterglow and afteremission seems to be clear confirming photon-stimulated origin of the phenomenon. Long component τ_2 of the afteremission cannot be attributed to direct photon-stimulated emission of electrons. It is likely that this component appears as the results of multiple electron retrapping process. Similar effect was observed in afteremission of pre-irradiated rare-gas solids [38].

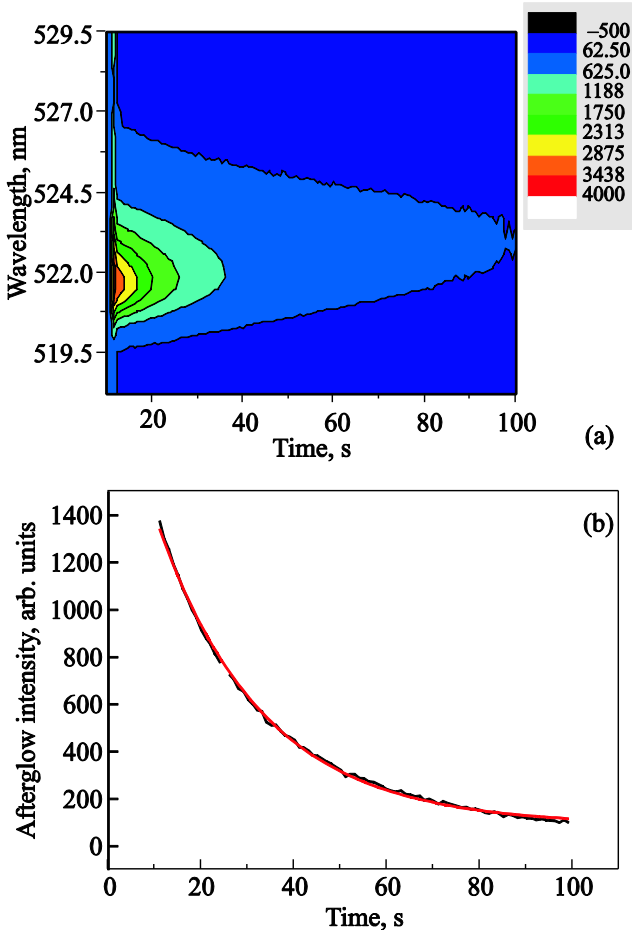

Fig. 3. Afterglow of nitrogen film detected on the $^2D \rightarrow {}^4S$ atomic transition (a) and its exponential fit (b).

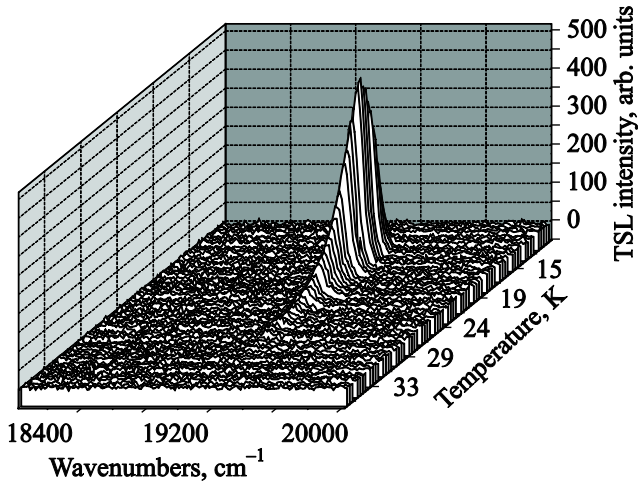

Fig. 4. 3D plot of TSL in the range of the $^2D \rightarrow {}^4S$ transition.

Figure 4 demonstrates TSL from pre-irradiated solid nitrogen measured in the range of the $^2D \rightarrow {}^4S$ transition at the warm-up with a constant rate 3.2 K/min (so-called linear regime). The TSL yield shows a peak near 16 K and wide shoulder between 20 and 30 K. In order to make comparison with temperature behavior of pressure more clear, we present 2D cut curves shown in Fig. 4 made perpendicular to the wavenumber axis. It indicates the temperature dependence of the TSL at a chosen wavenumber, that is of selected spectral line. Such a cut for 522 nm together with corresponding pressure curve is presented in Fig. 5. Increase in the spectrally resolved TSL intensity distinctly correlates the pressure enhancement and ALTpD feature falls within the range of the TSL glow curve. Considering that the ionization potential I of N atom is $I = 14.53$ eV that is lower than that of nitrogen molecule ($I = 15.58$ eV) [39] one could expect the formation of N^+ cations in irradiated solid nitrogen. N^+ centers formed under electron beam survive on completing irradiation. Upon warm-up they are neutralized by detrapping electrons by the reaction (1). Neutralization results in population of

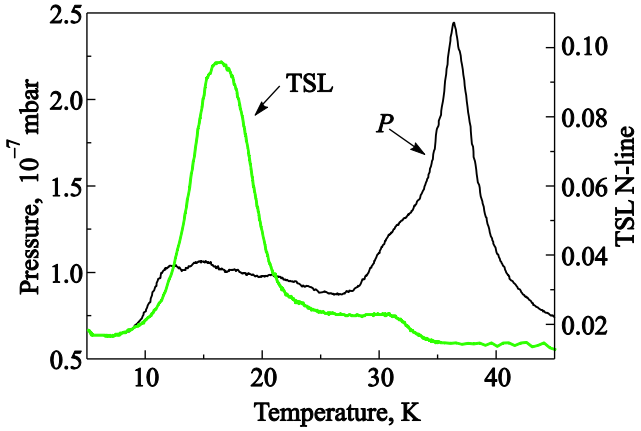

Fig. 5. Comparison of glow curve detected on the $^2D \rightarrow {}^4S$ atomic transition and pressure behavior upon warm-up of the pre-irradiated nitrogen film.

highly excited states followed by relaxation to the ^2D state and its decay with the α-line emission:

$$N^+ + e^- \rightarrow N^{**} \rightarrow N^*(^2D) \rightarrow N(^4S) + h\nu . \qquad (1)$$

Taking into account that strong molecular emissions from solid nitrogen were observed in vacuum ultraviolet VUV range [40–42] under excitation by an electron beam we performed measurements of thermally stimulated luminescence in the range of strongest singlet–singlet transition $a'\,^1\Sigma_u^- \rightarrow X^1\Sigma_g^+$. The TSL was detected at wavelengths corresponding transitions from zero vibrational level of the $a'\,^1\Sigma_u^-$ state to a number of vibrational levels of the ground state $X^1\Sigma_g^+$. Figure 6 presents as an example TSL glow curve recorded on the $a'\,^1\Sigma_u^-(0) \rightarrow X^1\Sigma_g^+(5)$ molecular transition together with the pressure curve. At low temperatures between 12 and 20 K the ALTpD curve follows the molecular emission indicating similarity of processes underlying these phenomena. Peak at 27 K observed in molecular TSL does not show itself neither in the pressure curve nor in the TSEE yield (Fig. 1). The most probable reason could be the fact that TSL contains contributions from both bulk and surface centers while TSEE and desorption characterize surface and subsurface layer. High-temperature peak appears close to the temperature range where deep layers of sample close to the sample–substrate interface become available due to sublimation. The pressure then drops sharply approaching the base value in the chamber indicating the sample loss.

First of all it should be stressed that the VUV TSL is observed on the molecular system with the dissociation limit which is formed by two nitrogen atoms in excited states: $N(^2D)$ + $N(^2D)$ that exclude population of the $a'\,^1\Sigma_u^-$ state via atom–atom recombination at low temperatures. Thus an appearing this molecular emission in TSL is caused by neutralization reaction that needs to be explained. The TSL of this kind occurrence supposes localized character of positive charge carriers in solid nitrogen

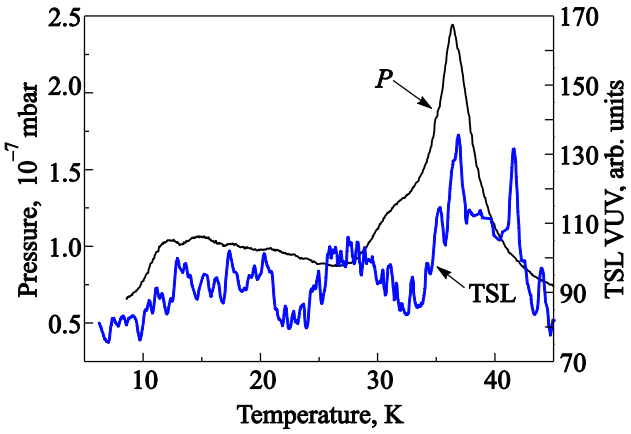

Fig. 6. Comparison of glow curve detected on the $a'^1\Sigma_u^- \rightarrow X^1\Sigma_g^+$ molecular transition and pressure behavior upon warm-up of the pre-irradiated nitrogen film.

that is in agreement with their low mobility [43]. Self-trapping of holes by the reaction

$$N_2^+ + N_2 \rightarrow (N_2)_2^+ \qquad (2)$$

similar to known in rare-gas solids [44] was suggested as one of the mechanisms underlying desorption induced by electronic transitions DIET from solid nitrogen [13]. The energy release in the neutralization reaction of self-trapped hole

$$(N_2)_2^{+v} + e^- \rightarrow N_2^* + N_2 + \Delta E \qquad (3)$$

was estimated as $\Delta E \approx 1$–3.7 eV [13].

In contrast to DIET for post-desorption starting state of $(N_2)_2^+$ for reaction (3) is vibrationally relaxed ground state of N_4^+. Neutralization of N_4^+ results in population of excited N_4^* molecular states. Relaxation could occur via transition structures for fragmentation [45]. For singlet state relaxation terminates in the lowest singlet excited state $a'\,^1\Sigma_u^-$ which then decays radiatively. The energy release in reaction (3) at $v = 0$ could be considered as a source of energy needed for post-desorption. Further experiments with measurements of partial desorption yields and determination of kinetic energies of desorbing particles are necessary to pinpoint in detail relaxation cascades.

Summary

The results of experiments on "post-desorption" from the surface of α-phase solid nitrogen preliminary irradiated by an electron beam are presented. Relaxation processes were monitored using a combination of activation spectroscopy methods — spectrally resolved thermally stimulated luminescence, thermally stimulated exoelectron emission — with measurement of the post-desorption yield. We have found a correlation of TSL, TSEE and post-desorption yields from solid nitrogen previously subjected to an electron beam. This suggests a relation between electron-positively charged centers recombination and low-temperature desorption processes. Analysis of the yields correlation enabled us to suggest a two-stage mechanism of the ALTpD: (i) thermally assisted release of electrons from their traps followed by (ii) charge recombination resulting in an energy release followed by its conversion into the kinetic energy of nitrogen particles and their ejection from the surface.

The authors cordially thank Profs. Peter Feulner and Roman Pedrys for helpful discussions. E.S., I.Kh. and S.U. thank Deutsche Forschungsgemeinschaft for the travel grant.

1. A.V. Dolbin, V.B. Esel'son, V.G. Gavrilko, V.G. Manzhelii, S.N. Popov, and N.A. Vinnikov, *Fiz. Nizk. Temp.* **36,** 465 (2010) [*Low Temp. Phys.* **36,** 365 (2010)].

2. Guido W. Fuchs, Kinsuk Acharyya, Suzanne E. Bisschop, Karin I. Oeberg, Fleur A. van Broekhuizen, Helen J. Fraser, Stephan Schlemmer, Ewine F. van Dishoeck, and Harold Linnartz, *Faraday Discussions* **133,** 331 (2006).
3. H. Schlichting and D. Menzel, *Surf. Sci.* **272**, 27 (1992).
4. W. Frieß, H. Schlichting, and D. Menzel, *Phys. Rev. Lett.* **74**, 1147 (1995).
5. G.J. Szulczewski and J.M. White, *J. Vacuum Sci. Technol. A: Vacuum, Surfaces, and Films* **15**, 1526 (1997).
6. F. Bartolucci and R. Franchy, *Surf. Sci*. **368**, 27 (1996).
7. H. Hopster and H. Ibach, *Surf. Sci*. **77**, 109 (1978).
8. B. Tränkenschuh, N. Fritsche, T. Fuhrmann, C. Papp, J.F. Zhu, R. Denecke, and H.-P. Steinrück, *J. Chem. Phys.* **124**, 074712 (2006).
9. W.X. Huang and J.M. White, *Surf. Sci.* **529,** 455 (2003).
10. Yu.G. Ptushinski, *Fiz. Nizk. Temp*. **30,** 3 (2004) [*Low Temp. Phys*. **30,** 1 (2004)].
11. Mark P. Collings, Mark A. Anderson, Rui Chen, John W. Dever, Serena Viti, David Williams, and Martin R.S. McCoustra, *Mon. Not. R. Astron. Soc*. **354,** 1133 (2004).
12. Alexander G.G.M. Tielens and Louis J. Allamandola, Chapter 11: "*Cool Interstellar Physics and Chemistry*" in *Physics and Chemistry at Low Temperatures*, Leonid Khriachtchev (ed.), Pan Stanford Publishing (2011), p. 341.
13. R.E. Johnson and J. Schou, *Mat. Fys. Medd. Dan. Vid. Selsk*. **43**, 403 (1993).
14. Robert E. Johnson, Robert W. Carlson, Timothy A. Cassidy, and Marcelo Fama, *Sputtering of Ices in the Science of Solar System Ices*, M.S. Gudipati and J. Castillo-Rogez (eds.), *Astrophysics and Space Science Library* **356**, Springer Science and Business Media, New York (2012).
15. O. Ellegard, J. Schou, H. Sorensen, and P. Borgesen, *Surf. Sci*. **167,** 474 (1986).
16. R. Pedrys, D.J. Oostra, A. Haring, A.E. Devries, and J. Schou, *Rad. Effects and Defects in Solids* **109,** 239 (1989).
17. E. Hudel, E. Steinacker, and P. Feulner, *Surf. Sci*. **273,** 405 (1992).
18. O. Rakhovskaia, P. Wiethoff, and P. Feulner, *Nucl. Instr. and Meth. B* **101,** 169 (1995).
19. H. Shi, P. Cloutier, and L. Sanche, *Phys. Rev. B* **52**, 5385 (1995).
20. M. Caron, H. Rothard, and A. Clouvas, *Surf. Sci*. **528,** 103 (2003).
21. F.L. Rook, R.E. Johnson, and W.L. Brown, *Surf. Sci*. **164,** 625 (1985).
22. W.L. Brown and R.E. Johnson, *Nucl. Instr. and Meth. B* **13**, 295 (1986).
23. O. Ellegard, J. Schou, B. Stenum, H. Sorensen, R. Pedrys, B. Warczak, D.J. Oostra, A. Haring, and A.E. Devries, *Surf. Sci.* **302**, 371 (1994).
24. O. Ellegard, J. Schou, H. Sorensen, R. Pedrys, and B. Warczak, *Nucl. Instr. and Meth. B* **78,** 192 (1993).
25. V. Balaji, D.E. David, R. Tian, J. Michl, and H.M. Urbassek, *J. Phys. Chem.* **99**, 15565 (1995).
26. B. Stenum, O. Ellegaard, J. Schou, H. Sorensen, and R. Pedrys, *Nucl. Instr. and Meth. B* **58,** 399 (1991).
27. R. Zehr, C. French, B.C. Haynie, A. Solodukhin, and I. Harrison, *Surf. Sci*. **451,** 76 (2000).
28. K.I. Öberg, E.F. van Dishoeck, and H. Linnartz, *Astron. Astrophys*. **496,** 281 (2009).
29. E.V. Savchenko, O.N. Grigorashchenko, G.B. Gumenchuk, A.G. Belov, E.M. Yurtaeva, I.V. Khyzhniy, M. Frankowski, M.K. Beyer, A.M. Smith-Gicklhorn, and V.E. Bondybey, *J. Low Temp. Phys*. **126**, 621 (2005).
30. Alexey Ponomaryov, Galina Gumenchuk, Elena Savchenko, and Vladimir E. Bondybey, *Phys. Chem. Chem. Phys*. **9**, 1329 (2007).
31. E.V. Savchenko, I.V. Khyzhniy, S.A. Uyutnov, G.B. Gumenchuk, A.N. Ponomaryov, G. Zimmerer, and V.E. Bondybey, *Nucl. Instr. and Meth. B* **267,** 1733 (2009).
32. E.V. Savchenko, I.V. Khyzhniy, S.A. Uyutnov, G.B. Gumenchuk, A.N. Ponomaryov, and V.E. Bondybey, *Nucl. Instr. and Meth. B* **268,** 3239 (2010).
33. A.N. Ponomaryov, E.V. Savchenko, G.B. Gumenchuk, I.V. Khizhniy, M. Frankowski, and V.E. Bondybey, *Fiz. Nizk. Temp*. **33,** 705 (2007) [*Low Temp. Phys*. **33,** 532 (2007)].
34. I. Khyzhniy, E. Savchenko, S. Uyutnov, G. Gumenchuk, A. Ponomaryov, and V. Bondybey, *Rad. Meas*. **45**, 353 (2010).
35. G. Bader, G. Perluzzo, L.G. Caron, and L. Sanche, *Phys. Rev. B* **30,** 78 (1984).
36. V.G. Storchak, D.G. Eshchenko, J.H. Brewer, S.P. Cottrell, S.F.J. Cox, E. Karlsson, and R.W. Wappling, *J. Low Temp. Phys*. **122,** 527 (2001).
37. A. Lofthus and P.H. Krupenie, *J. Phys. Chem. Ref. Data* **6**, 113 (1977).
38. E.V. Savchenko, I.V. Khyzhniy, S.A. Uyutnov, G.B. Gumenchuk, A.N. Ponomaryov, M.K. Beyer, and V.E. Bondybey, *J. Phys. Chem. A* **115,** 7258 (2011).
39. NIST Chemistry WebBook http://webbook.nist.gov/chemistry/.
40. Ya. Fugol', Yu.B. Poltoratskii, and E.V. Savchenko, *JETP Lett*. **24,** 1 (1976).
41. F.A. Coletti and A.M. Bonnot, *Chem. Phys. Lett*. **45,** 580 (1977).
42. Yu.B. Poltoratskii, V.M. Stepanenko, and I.Ya. Fugol', *Fiz. Nizk. Temp*. **7,** 121 (1981) [*Sov. J. Low Temp. Phys*. **7,** 60 (1981)].
43. R.J. Loveland, P.G. Le Comber, and W.E. Spear, *Phys. Rev. B* **6,** 3121 (1972).
44. K.S. Song and R.T. Williams, *Self-Trapped Excitons*, Springer Series in Solid State Science, Vol. 105, Springer-Verlag, Berlin (1996).
45. M.T. Nguyen, *Coord. Chem. Rev*. **244**, 93 (2003).